Applied Physics Letters

RESEARCH ARTICLE | JULY 09 2024

Coupled vertical double quantum dots at single-hole occupancy

Alexander S. Ivlev ; Hanifa Tidjani ; Stefan D. Oosterhout ; Amir Sammak; Giordano Scappucci ; Menno Veldhorst

Appl. Phys. Lett. 125, 023501 (2024)
https://doi.org/10.1063/5.0198274

Applied Physics Letters ARTICLE pubs.aip.org/aip/apl

Coupled vertical double quantum dots at single-hole occupancy

Cite as: Appl. Phys. Lett. **125**, 023501 (2024); doi: 10.1063/5.0198274
Submitted: 17 January 2024 · Accepted: 20 June 2024 ·
Published Online: 9 July 2024

Alexander S. Ivlev,[1,a] Hanifa Tidjani,[1] Stefan D. Oosterhout,[2] Amir Sammak,[2] Giordano Scappucci,[1] and Menno Veldhorst[1,a]

AFFILIATIONS

[1]QuTech and Kavli Institute of Nanoscience, Delft University of Technology, PO Box 5046, 2600 GA, Delft, The Netherlands
[2]QuTech and Netherlands Organisation for Applied Scientific Research (TNO), Delft, The Netherlands

[a]Authors to whom the correspondence should be addressed: a.s.ivlev@tudelft.nl and m.veldhorst@tudelft.nl

ABSTRACT

Gate-defined quantum dots define an attractive platform for quantum computation and have been used to confine individual charges in a planar array. Here, we demonstrate control over vertical double quantum dots confined in a strained germanium double quantum well. We sense individual charge transitions with a single-hole transistor. The vertical separation between the quantum wells provides a sufficient difference in capacitive coupling to distinguish quantum dots located in the top and bottom quantum wells. Tuning the vertical double quantum dot to the (1,1) charge state confines a single-hole in each quantum well beneath a single plunger gate. By simultaneously accumulating holes under two neighboring plunger gates, we are able to tune to the (1,1,1,1) charge state. These results motivate quantum dot systems that exploit the third dimension, opening new opportunities for quantum simulation and quantum computing.

Attaining control over individual charges in silicon[1–3] and germanium[4–6] constituted a necessary prerequisite to enable quantum computation with gate-defined quantum dots.[7,8] Planar quantum dot systems have progressed significantly, supporting high-fidelity single and two-qubit logic, multi-qubit logic, rudimentary error correction, and control over a 16 quantum dot array.[9–17] The development of a double germanium quantum well heterostructure[18] has enabled the realization of a vertically coupled double quantum dot[19] by taking advantage of the third dimension. Gaining control over single charges confined in quantum dots in multilayer systems may become a key asset in obtaining high-connectivity in large quantum dot arrays.[19] In the near term, single-charge control in bilayer quantum dot systems may enable the realization of small-scale quantum simulators of magnetic phases in correlated spin systems.[20]

Here, we demonstrate a vertical double quantum dot formed under a single plunger gate and tuned to single-hole occupancy. The occupancy is detected by charge sensing with a single-hole transistor. Using a second plunger gate, the system is extended to a vertical 2×2 quantum dot array in the x-z plane-parallel to the (100) heterostructure growth direction, filled down to the (1,1,1,1) hole occupation. In comparison, achieving such a charge configuration in planar systems is non-trivial and has been demonstrated only recently in planar germanium[21] and silicon.[22]

Figure 1(a) depicts a schematic of the Ge/SiGe heterostructure, grown by reduced pressure chemical vapor deposition as detailed in Tosato *et al.*[18] The heterostructure features two strained Ge quantum wells with thicknesses of 16 and 10 nm embedded in strain-relaxed $Si_{0.2}Ge_{0.8}$. The separation between the quantum wells is 4 nm, and the separation of the top quantum well from the semiconductor–dielectric interface is 55 nm, in line with current heterostructures[23] hosting spin qubit devices. Ti/Pd metallic gates [Fig. 1(b)] are fabricated in two layers and separated by Al_2O_3, to electrostatically confine holes in the quantum wells (for further details on fabrication, see Ref. 19). Four plunger gates are patterned, with the left-most plunger gate SL_P forming a charge sensor and the right-most acting only as a reservoir in this experiment. The barrier gates $SL_{N(S)}$ control the tunneling between the charge sensor and the Ohmic contacts. We define quantum dots localized in the two quantum wells using plunger gates P_L and P_R and barrier gates B_L, B_C, and B_R. Additionally, screening gates SC_L and SC_R provide further fine-tuning and prevent the formation of unwanted quantum dots. Barrier gates B_L and B_R also control the loading of charge carriers from the reservoirs to the quantum dots.

To facilitate charge sensing, a 100 μV bias is applied across the Ohmic contacts S and D. The current signal through the sensor is determined by two-terminal DC measurements using low impedance lines and resulting in an integration time on the order of 100 μs. We

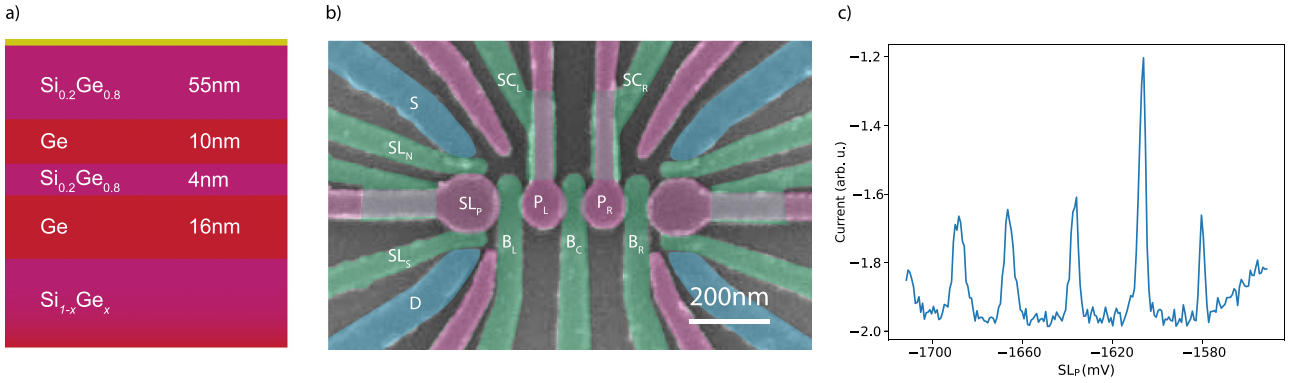

FIG. 1. Double quantum well heterostructure and top gate layout. (a) Schematic of the double quantum well heterostructure with the numbers indicating the targeted layer thickness. The yellow layer denotes the native SiOx. (b) False colored SEM of a device nominally identical to the one used in this experiment. The left-most plunger gate acts as a charge sensor, and the two central plunger gates and surrounding barrier gates confine individual holes under $P_{L,R}$. The remaining right side of the device forms a hole-reservoir. (c) Typical Coulomb oscillations of the single-hole transistor formed underneath the plunger gate SL_P, at a typical source-drain bias of 100 μV.

calibrate the gate voltages to observe well-defined Coulomb peaks corresponding to the transport of holes through the single-hole transistor (SL_P), as seen in Fig. 1(c). At the edge of a Coulomb peak, the source–drain current is highly sensitive to the electrostatic environment and, in particular, to the charge occupation of any quantum dots under plunger gates P_L and P_R, similar to charge sensors in single quantum well systems. During all following measurements, the voltage on SL_P is tuned such that it maintains a high sensitivity to the studied charge states. Previous works have observed that the transport signal through a single-hole transistor may be diminished in a double quantum dot regime;[19] therefore, we carefully tune the sensor to obtain regular and well-defined Coulomb peaks. We speculate that in this regime, only one quantum well is contributing to transport through the charge sensor (see supplementary material II).

The charge sensor SL_P effectively detects the charge state beneath the plunger P_L. We begin by accumulating under P_L, while keeping P_R depleted, in order to avoid a lateral double quantum dot signature. Using P_L and B_C, we tune to a double dot regime under P_L and control the occupation of the two quantum dots QD_{L1} and QD_{L2}. Given their strong coupling to P_L, it is likely the dots are positioned underneath P_L. To achieve orthogonal control of the charge occupation in the quantum dots, we construct a virtual gate matrix, which couples QD_{L1} to vP_L, and QD_{L2} to vB_C. This is enabled by a difference in the lever arm ratio $\alpha_{L1,BC}/\alpha_{L1,PL} < \alpha_{L2,BC}/\alpha_{L2,PL}$, where $\alpha_{D,G}$ is the lever arm between gates G and quantum dot D. As a result, we can construct virtual gates vP_L and vB_C (Fig. 2) to obtain independent control of the loading onto each quantum dot, down to the single-hole regime. The linearly defined virtual gate space is effective in a small voltage regime but is insufficient to virtualize subsequent transitions of the double quantum dot under P_L [Fig. 2(a)]. In particular, the transitions of QD_{L2} have a strongly varying lever arm across consecutive occupations. This difference between the quantum dots can be explained by a weaker in-plane confinement of QD_{L2}, which is consistent with it being located in the bottom quantum well.

To establish that each quantum dot is, indeed, located in a distinct quantum well, we qualitatively estimate the location of both quantum dots. This is done by extracting the lever arm ratios of the surrounding gates to each quantum dot from the charge-stability diagrams, similar to the method used by Tidjani *et al.*[19] We find that the two quantum dots have approximately equal coupling to the two surrounding barrier gates B_L and B_C. In particular, we determine $\alpha_{L1,BC}/\alpha_{L1,PL} \approx \alpha_{L1,BL}/\alpha_{L1,PL} \approx 1.0$ and $\alpha_{L2,BC}/\alpha_{L2,PL} \approx \alpha_{L2,BL}/\alpha_{L2,PL} \approx 1.6$ (see supplementary material III) for the corresponding charge-stability diagrams. These lever arms indicate that both quantum dots are equidistant in position between B_L and B_C. We note that B_L and B_C have similar shape and are fabricated in the same layer, and we, therefore, ignore geometric effects. On the other hand, $\alpha_{L1,SC_L}/\alpha_{L1,PL} \approx \alpha_{L2,SC_L}/\alpha_{L2,PL} \approx 0.4$ indicates that neither quantum dot is significantly closer to SC_L.

Together, these findings suggest that the quantum dots are vertically stacked beneath plunger gate P_L. Since the quantum dots are well-defined with a distinct interdot transition and charge signal to the sensor, we conclude that they are separated in the z-direction, with each quantum well confining one quantum dot. We assign QD_{L2} to the bottom quantum well as its relative coupling to the barrier gates is larger than that of QD_{L1}, which has a stronger in-plane confinement.[19] Moreover, an interdot transition $(N_{L1}, N_{L2}+1) \rightarrow (N_{L1}+1, N_{L2})$ is induced by applying an increasingly negative P_L voltage, indicating that QD_{L1} is located closer to P_L. The vertically coupled double quantum dot is visualized in Fig. 2(b).

Our conclusions are further supported by our finding of comparable results for the two quantum dots QD_{R1} and QD_{R2} under P_R, which we also tune to the (1,1) regime and where we similarly argue that each quantum dot is located in a different quantum well underneath P_R (supplementary material IV). This reproducibility bodes well for future efforts in operating larger arrays.

The observation of a distinct $(1,0)-(0,1)$ interdot transition line in the right panel of Fig. 2(a) indicates a distinct capacitative coupling between each quantum dot and SL_P. This distinct capacitive coupling is encouraging, since the current heterostructure has a modest inter-layer separation, suggesting potential for further enhancement. The current ability to distinguish in which quantum well a charge is located is holds promise for vertical Pauli spin-blockade (PSB) readout. This gives perspective for the integration of a readout ancilla that can be used for PSB directly underneath or above a data qubit. This distinguishability furthermore allows to better study the inter-layer tunnel

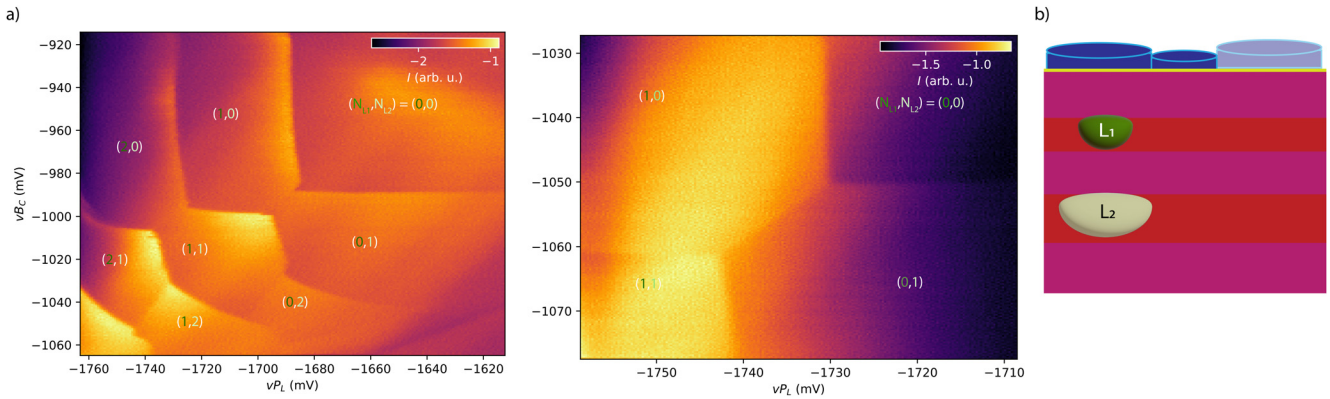

FIG. 2. Single-hole occupancy in a vertical double quantum dot. (a) The left panel shows the charge-stability diagram of a double quantum dot formed underneath plunger gate P_L measured by charge sensing. The occupation (N_{L1}, N_{L2}) for quantum dots QD_{L1} and QD_{L2} is noted in each region and is controlled by the gate voltages on P_L and B_C, which are applied as virtual gates $vP_L = P_L - 0.55B_C - 0.2SL_P$ and $vB_C = -0.9P_L + B_C - 0.18SL_P$ to maintain visibility of the charge sensor. In the right panel, we focus on the (1,0)–(0,1) transition. The charge sensor is optimized to distinguish the interdot transition. Here, the virtual gate definition is set to $vP_L = P_L - 0.58B_C - 0.18SL_P$ and $vB_C = -0.95P_L + B_C - 0.14SL_P$. The gate voltages at the center of the right panel are $P_L = -1381$ mV and $B_C = -183$ mV. (b) Schematic depicting the double occupation under P_L, while P_R is kept below the accumulation voltage.

coupling itself. The control over the coupling between the quantum wells may be limited and largely predefined by their separation. Nonetheless, controlling the quantum dot occupation may serve as means to discretely change the tunnel coupling due to the varying wavefunction densities of different orbitals. The appreciable difference in the lever arms of the gates to the quantum dots furthermore suggests gate-based tunability of the inter-layer tunnel coupling and exchange interaction. An applied gate voltage could shift the quantum dots relative to one another, allowing to decrease their overlap and reducing the tunnel coupling. Alternatively, the gate voltage could influence the penetration of the wavefunction into the SiGe barrier. However, a more systematic study is needed to understand to which extent the charge occupation and tunnel couplings can be tuned independently *in situ*.

Having established individual control over the double quantum dots underneath each plunger gate, we now focus on simultaneous control over the hole occupation under both plungers to demonstrate a 2×2 array in the x-z plane. Starting in the few hole regime under P_R, we maintain the (1,1) P_R occupation and tune the system toward the voltage regime in which both quantum dots under P_L become occupied with a single-hole. The left (right) panel of Fig. 3(a) demonstrates the charge-stability diagram of $vP_{L(R)}$ vs vB_C. In each diagram,

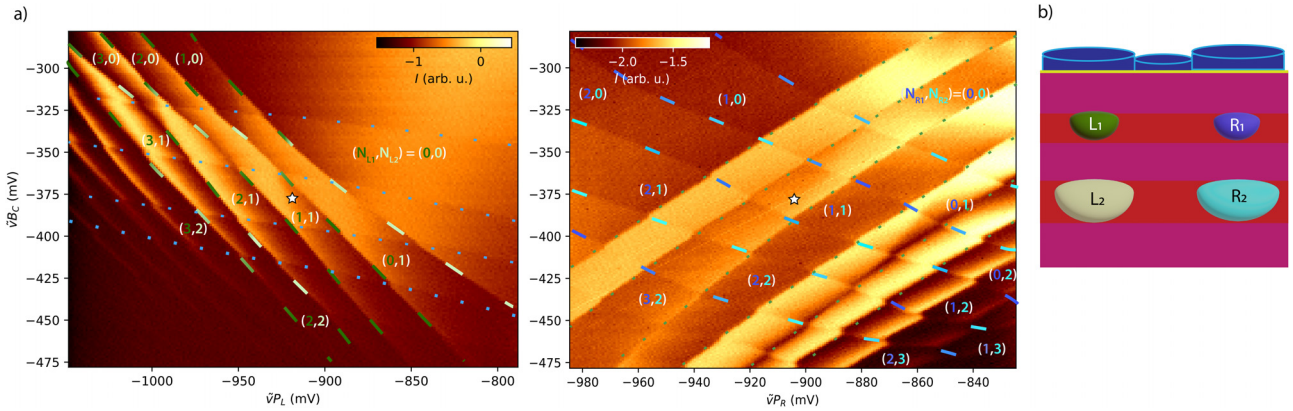

FIG. 3. Single-hole occupancy in two coupled vertical double quantum dots. (a) The left panel shows the charge-stability diagram with individual transitions of the double quantum dot underneath P_L, where dark (light) dashed green lines correspond to reservoir transitions of $QD_{L1(2)}$, serving as a guide to the eye. In addition, the blue dotted transitions correspond to the double quantum dot under P_R. We note that the individual quantum dots are poorly distinguishable due to the small lever arm differences between P_L and the quantum dots underneath P_R. The occupation of the top (bottom) quantum well under P_L $N_{L1(2)}$ is indicated in the different regions. The right panel similarly shows the charge-stability diagram with individual transitions of the double quantum dot underneath P_R, with the transition to $QD_{R1(2)}$ indicated with dark (light) blue. The transitions corresponding to the double quantum dot under P_L are indicated with a dotted green line. Again, the occupation of the top (bottom) quantum wells under P_R is indicated with $N_{R1(2)}$. In both subfigures, the virtual gate voltages are $\tilde{v}\ P_L = P_L - 0.2P_R - 0.17SL$ and $\tilde{v}\ B_C = B_C - 0.22SL$ and $\tilde{v}\ P_R = P_R - 0.4P_L - 0.5B_C - 0.075SL$. To capture multiple transitions of the sensor in the right panel of (a), the signal is averaged over multiple datasets at different sensor voltages SL_P. The stars correspond to the same voltage values and give the location of the (1,1,1,1) charge state. (b) Schematic depicting the 2×2 array. The colors match the transitions in (a).

one can distinguish the double quantum dot under its corresponding plunger gate as well as additional transitions corresponding to the double quantum dot under the other plunger gate. In this figure, the upper and lower quantum dots are not virtualized with respect to each other as with in Fig. 2(a), in order to obtain a four quantum dot charge-stability diagram while only varying two plunger gates. In the middle of the measurement range, the vertical 2×2 array is in the (1,1,1,1) charge occupation, depicted in Fig. 3(b). In this regime, it becomes more challenging to distinguish individual transitions from each quantum dot due to the noticeably increased inter-layer tunnel coupling between QD_{L1} and QD_{L2} (see supplementary material V for an analysis of the capacitive and tunnel couplings). This increased coupling is thought to result from the central barrier voltage being increased to $B_C = 13\,\text{mV}$, compared to $B_C = -182\,\text{mV}$ in Fig. 2, which increases the in-plane confinement. Increasing B_C was necessary to achieve the desired (1,1,1,1) charge state. This high B_C voltage, moreover, reduces the intralayer capacitive and tunnel coupling, consistent with the observed small interdot transitions between the P_L and P_R quantum dots (see supplementary material V).

In conclusion, we have established single-hole charge control over quantum dots in a double quantum well. A significant challenge remains in obtaining control over the interdot coupling and, in particular, when the coupling is inter-layer, since the gates controlling the occupation also control the coupling. Despite this, we have shown that even in a strongly coupled system, charge sensing and orthogonal control of quantum dots in each quantum well are possible, through the construction of virtual gate matrices. Furthermore, we have demonstrated a 2×2 quantum dot array oriented perpendicular to the quantum well plane and tuned to the (1,1,1,1) charge state. Small extensions in the system size, such as a $2 \times 2 \times 2$ quantum dot array, may allow the study of intriguing physics arising in bilayer Hubbard models.[20] Moreover, the ability to control single charges in multilayer systems may facilitate high-connectivity semiconductor quantum processors.

See the supplementary material for details on the experimental setup and the regime the charge sensor is in. We also provide data allowing us to triangulate the vertical double quantum dots under P_L as well as P_R. Finally, we analyze several anti-crossings of the charge-stability diagrams to give a crude assessment of the capacitive and tunnel couplings between the quantum dots.

We thank Sander de Snoo for software development and Alberto Tosato and Corentin Déprez for useful discussions. We acknowledge support through a Dutch Research Council (NWO) Domain Science (ENW) Grant and a European Research Council (ERC) Starting Grant QUIST (850641).

AUTHOR DECLARATIONS

Conflict of Interest

At the time of publication A.S. is employed by Equal1 Laboratories (The Netherlands) B.V. The remaining authors declare no competing interest.

Author Contributions

Alexander S. Ivlev and Hanifa Tidjani contributed equally to this study.

Alexander S. Ivlev: Conceptualization (equal); Formal analysis (lead); Investigation (lead); Methodology (equal); Validation (equal); Visualization (equal); Writing – original draft (equal); Writing – review & editing (equal). **Hanifa Tidjani:** Conceptualization (equal); Formal analysis (lead); Investigation (lead); Methodology (equal); Validation (equal); Visualization (equal); Writing – original draft (equal); Writing – review & editing (equal). **Stefan D. Oosterhout:** Resources (lead). **Amir Sammak:** Resources (supporting). **Giordano Scappucci:** Resources (supporting); Supervision (supporting); Writing – review & editing (supporting). **Menno Veldhorst:** Conceptualization (equal); Funding acquisition (lead); Supervision (lead); Validation (equal); Writing – review & editing (equal).

DATA AVAILABILITY

The code, analysis, and raw data that support the findings of this study are openly available in a Zenodo at https://doi.org/10.5281/zenodo.10513179, Ref. 24.

REFERENCES

[1]S. J. Angus, A. J. Ferguson, A. S. Dzurak, and R. G. Clark, "Gate-defined quantum dots in intrinsic silicon," Nano Lett. **7**, 2051–2055 (2007).
[2]C. B. Simmons, M. Thalakulam, N. Shaji, L. J. Klein, H. Qin, R. H. Blick, D. E. Savage, M. G. Lagally, S. N. Coppersmith, and M. A. Eriksson, "Single-electron quantum dot in Si/SiGe with integrated charge sensing," Appl. Phys. Lett. **91**, 213103 (2007).
[3]F. A. Zwanenburg, A. S. Dzurak, A. Morello, M. Y. Simmons, L. C. L. Hollenberg, G. Klimeck, S. Rogge, S. N. Coppersmith, and M. A. Eriksson, "Silicon quantum electronics," Rev. Mod. Phys. **85**, 961–1019 (2013).
[4]N. W. Hendrickx, D. P. Franke, A. Sammak, M. Kouwenhoven, D. Sabbagh, L. Yeoh, R. Li, M. L. V. Tagliaferri, M. Virgilio, G. Capellini, G. Scappucci, and M. Veldhorst, "Gate-controlled quantum dots and superconductivity in planar germanium," Nat. Commun. **9**, 2835 (2018).
[5]W. I. L. Lawrie, H. G. J. Eenink, N. W. Hendrickx, J. M. Boter, L. Petit, S. V. Amitonov, M. Lodari, B. Paquelet Wuetz, C. Volk, S. G. J. Philips, G. Droulers, N. Kalhor, F. van Riggelen, D. Brousse, A. Sammak, L. M. K. Vandersypen, G. Scappucci, and M. Veldhorst, "Quantum dot arrays in silicon and germanium," Appl. Phys. Lett. **116**, 080501 (2020).
[6]G. Scappucci, C. Kloeffel, F. A. Zwanenburg, D. Loss, M. Myronov, J.-J. Zhang, S. De Franceschi, G. Katsaros, and M. Veldhorst, "The germanium quantum information route," Nat. Rev. Mater. **6**, 926–943 (2020).
[7]D. Loss and D. P. DiVincenzo, "Quantum computation with quantum dots," Phys. Rev. A **57**, 120–126 (1998).
[8]G. Burkard, T. D. Ladd, A. Pan, J. M. Nichol, and J. R. Petta, "Semiconductor spin qubits," Rev. Mod. Phys. **95**, 025003 (2023).
[9]J. Yoneda, K. Takeda, T. Otsuka, T. Nakajima, M. R. Delbecq, G. Allison, T. Honda, T. Kodera, S. Oda, Y. Hoshi, N. Usami, K. M. Itoh, and S. Tarucha, "A quantum-dot spin qubit with coherence limited by charge noise and fidelity higher than 99.9%," Nat. Nanotechnol. **13**, 102–106 (2018).
[10]W. I. L. Lawrie, M. Rimbach-Russ, F. v. Riggelen, N. W. Hendrickx, S. L. d. Snoo, A. Sammak, G. Scappucci, J. Helsen, and M. Veldhorst, "Simultaneous single-qubit driving of semiconductor spin qubits at the fault-tolerant threshold," Nat. Commun. **14**, 3617 (2023).
[11]N. W. Hendrickx, W. I. L. Lawrie, M. Russ, F. van Riggelen, S. L. de Snoo, R. N. Schouten, A. Sammak, G. Scappucci, and M. Veldhorst, "A four-qubit germanium quantum processor," Nature **591**, 580–585 (2021).
[12]S. G. J. Philips, M. T. M. Dzik, S. V. Amitonov, S. L. de Snoo, M. Russ, N. Kalhor, C. Volk, W. I. L. Lawrie, D. Brousse, L. Tryputen, B. P. Wuetz, A. Sammak, M. Veldhorst, G. Scappucci, and L. M. K. Vandersypen, "Universal control of a six-qubit quantum processor in silicon," Nature **609**, 919–924 (2022).
[13]X. Xue, M. Russ, N. Samkharadze, B. Undseth, A. Sammak, G. Scappucci, and L. M. K. Vandersypen, "Quantum logic with spin qubits crossing the surface code threshold," Nature **601**, 343–347 (2022).

[14]A. Noiri, K. Takeda, T. Nakajima, T. Kobayashi, A. Sammak, G. Scappucci, and S. Tarucha, "Fast universal quantum gate above the fault-tolerance threshold in silicon," Nature **601**, 338–342 (2022).
[15]K. Takeda, A. Noiri, T. Nakajima, T. Kobayashi, and S. Tarucha, "Quantum error correction with silicon spin qubits," Nature **608**, 682–686 (2022).
[16]F. van Riggelen, W. I. L. Lawrie, M. Russ, N. W. Hendrickx, A. Sammak, M. Rispler, B. M. Terhal, G. Scappucci, and M. Veldhorst, "Phase flip code with semiconductor spin qubits," npj Quantum Inf. **8**, 124 (2022).
[17]F. Borsoi, N. W. Hendrickx, V. John, M. Meyer, S. Motz, F. van Riggelen, A. Sammak, S. L. de Snoo, G. Scappucci, and M. Veldhorst, "Shared control of a 16 semiconductor quantum dot crossbar array," Nat. Nanotechnol. **19**, 21–27 (2023).
[18]A. Tosato, B. Ferrari, A. Sammak, A. R. Hamilton, M. Veldhorst, M. Virgilio, and G. Scappucci, "A high-mobility hole bilayer in a germanium double quantum well," Adv. Quantum Technol. **5**, 2100167 (2022).
[19]H. Tidjani, A. Tosato, A. Ivlev, C. Déprez, S. Oosterhout, L. Stehouwer, A. Sammak, G. Scappucci, and M. Veldhorst, "Vertical gate-defined double quantum dot in a strained germanium double quantum well," Phys. Rev. Appl. **20**, 054035 (2023).
[20]D. Buterakos and S. D. Sarma, "Magnetic phases of bilayer quantum-dot hubbard model plaquettes," Phys. Rev. B **108**, 235301 (2023).
[21]F. van Riggelen, N. W. Hendrickx, W. I. L. Lawrie, M. Russ, A. Sammak, G. Scappucci, and M. Veldhorst, "A two-dimensional array of single-hole quantum dots," Appl. Phys. Lett. **118**, 044002 (2021).
[22]F. K. Unseld, M. Meyer, M. T. Mądzik, F. Borsoi, S. L. de Snoo, S. V. Amitonov, A. Sammak, G. Scappucci, M. Veldhorst, and L. M. K. Vandersypen, "A 2D quantum dot array in planar 28Si/SiGe," Appl. Phys. Lett. **123**, 084002 (2023).
[23]M. Lodari, N. W. Hendrickx, W. I. L. Lawrie, T.-K. Hsiao, L. M. K. Vandersypen, A. Sammak, M. Veldhorst, and G. Scappucci, "Low percolation density and charge noise with holes in germanium," Mater. Quantum Technol. **1**, 011002 (2021).
[24]A. Ivlev, H. Tidjani, S. Oosterhout, A. Sammak, G. Scappucci, and M. Veldhorst (2024). "Data from: Coupled vertical double quantum dots at single-hole occupancy," Zenodo. https://doi.org/10.5281/zenodo.10513179